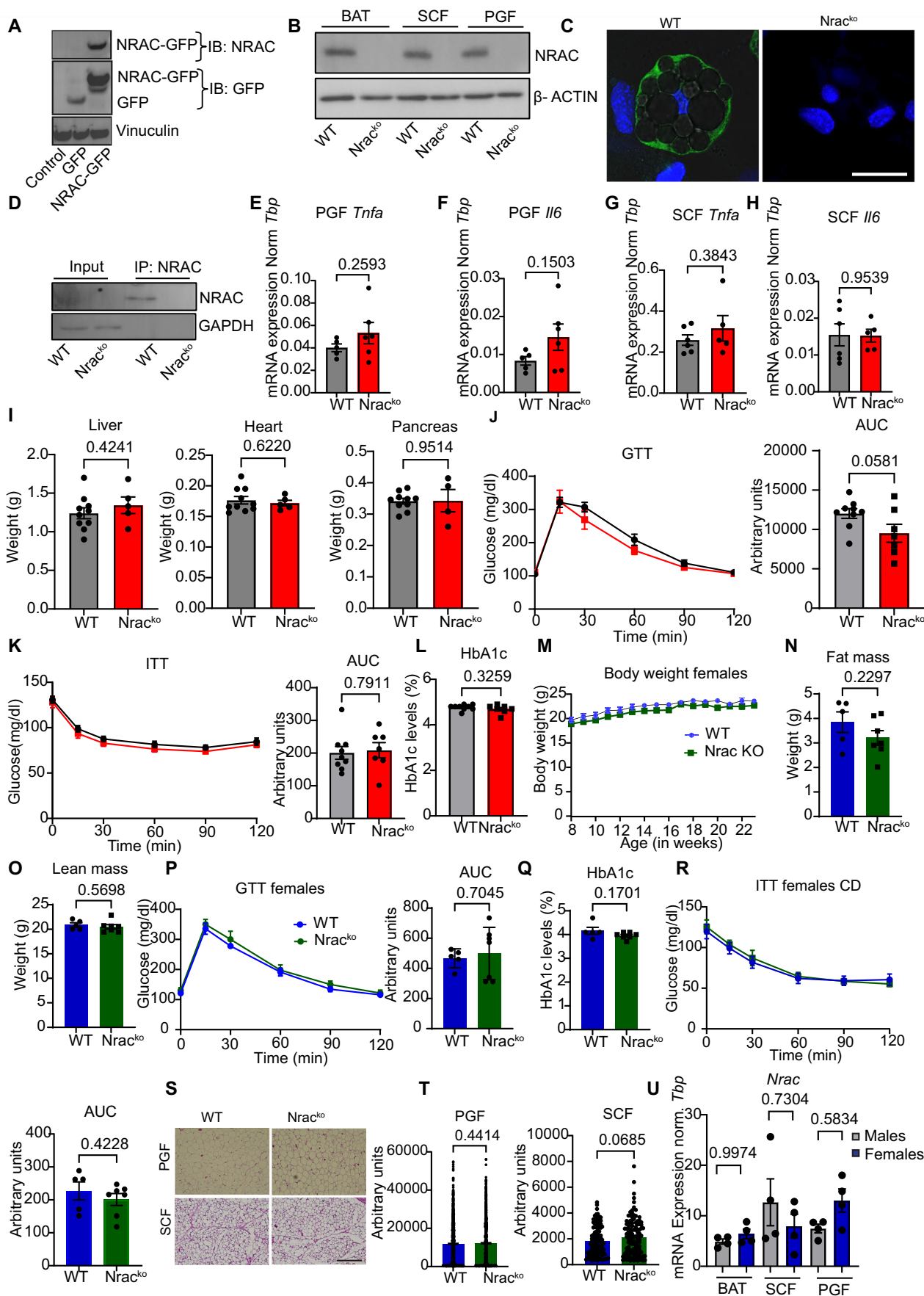
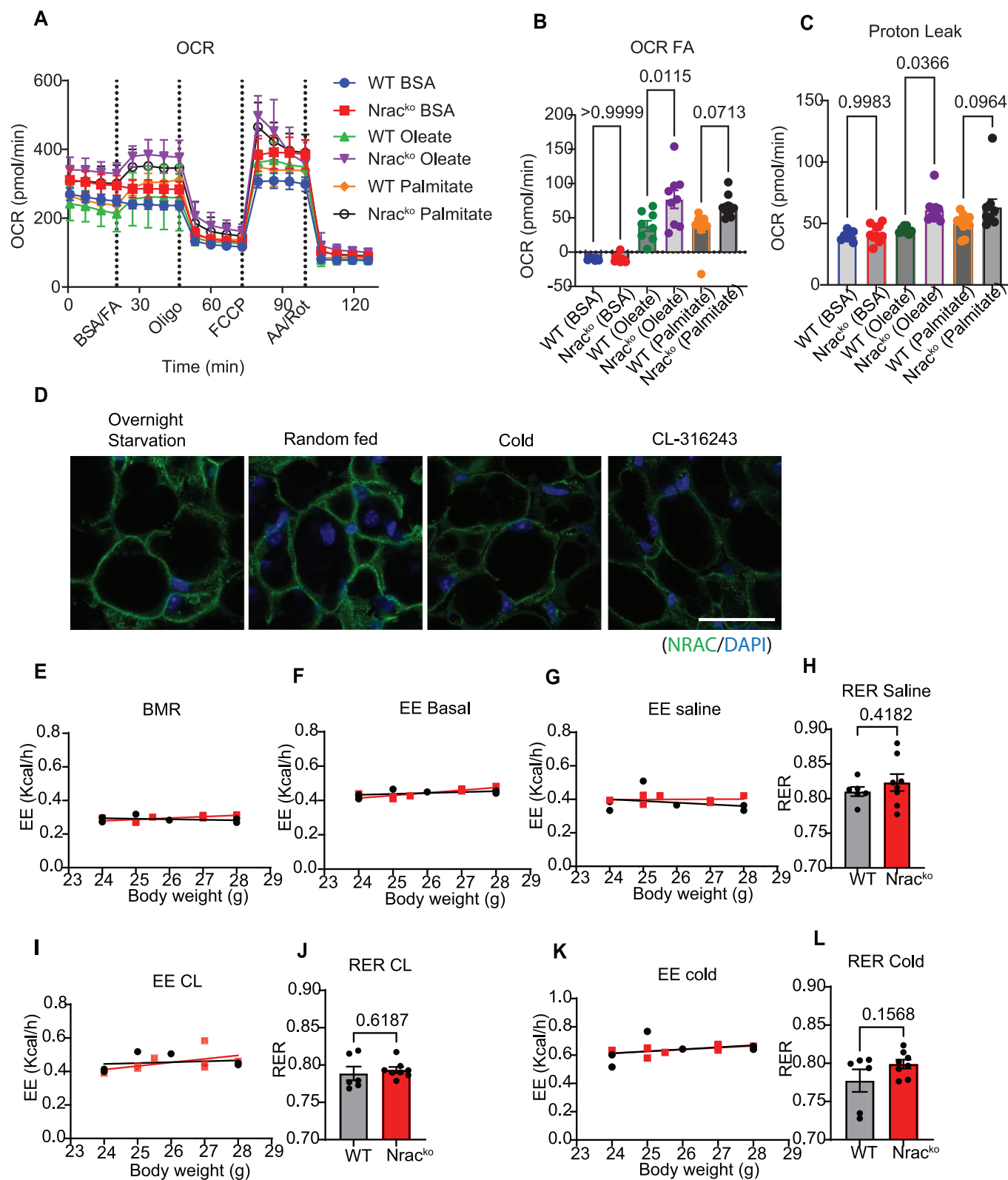


## Expanded View Figures

### Figure EV1. NRAC deletion does not affect glucose metabolism or insulin sensitivity in chow diet fed mice.

Validation of NRAC antibody by (A) western blotting of HEK293T cells transfected with either NRAC-GFP or GFP plasmids. Untransfected cells were used as control. (B) Western blotting to detect endogenous NRAC in BAT, SCF and PGF and (C) immunostaining of subcutaneous differentiated mature adipocytes to detect endogenous NRAC (scale bar 10  $\mu$ m), and (D) Immunoprecipitation of NRAC from perigonadal fat (PGF). (E–H) mRNA expression of *Tnfa* and *Il6* in PGF and SCF of male mice ( $n = 6$  wt, 5ko), (I) weights of liver, heart and pancreas ( $n = 9$  wt, 5ko). (J) Glucose tolerance test and area under the curve (age 8 weeks). (K) Insulin tolerance test (ITT) and area under the curve (AUC) in 9 weeks old male mice. (L) Percentage of HbA1c in 12-week-old male mice. (M) Body weight development of chow diet fed female wt and *Nrac*<sup>ko</sup> mice. (N) Fat and (O) lean mass of 15-week-old chow diet fed female mice. (P) Glucose tolerance test and area under the curve of 8 weeks old female mice. (Q) %HbA1c in 12-week-old female mice. (R) Insulin tolerance test (ITT) and area under the curve (AUC) in 9-week-old female mice. (S) H&E staining of SCF and PGF tissues of female mice (Age 23 weeks), and (T) quantification of lipid droplets.  $n = 9$ wt and 7ko for males and 5wt and 7ko for females. (U) mRNA expression of *Nrac* from BAT, SCF and PGF of male and female mice ( $n = 4$ ). Data are shown as mean  $\pm$  SEM. \* $P < 0.05$ , \*\* $P < 0.01$ , \*\*\* $P < 0.001$  by Student's *t* test or one or two-way ANOVA. Source data are available online for this figure.





**Figure EV2. NRAC deletion does not affect energy homeostasis, food intake and substrate utilization in mice under chow diet.**

(A) Oxygen consumption rates (OCR) in wt and *Nrac*<sup>ko</sup> differentiated adipocytes. Injection strategy included BSA or BSA conjugated oleate and palmitate (100  $\mu$ M each) (port 1), oligomycin (port 2), FCCP (port 3) and Antimycin A and rotenone in port 4. (B) OCR calculated by subtracting OCR after fatty acid (FA) stimulation from basal respiration. (C) Proton leak calculated by subtracting oligomycin OCR from non-mitochondrial OCR ( $n = 9$ ). (D) Immunostaining of BAT from wt mice either overnight starved (16 h), random fed, acute cold, (4 h) and CL-316243 injected mice ( $n = 3$ ), age 12 weeks (scale 100  $\mu$ m). (E) Basal metabolic rate (BMR). (F) Energy expenditure and respiratory exchange ratio (RER), (G, H) in saline treated mice, (I, J) in CL316243 treated mice and (K, L) upon acute cold exposure ( $n = 6$  WT and 8KO, Age 16 weeks). Data are shown as mean  $\pm$  SEM. \* $P < 0.05$ , \*\* $P < 0.01$ , \*\*\* $P < 0.001$  by Student's  $t$  test or one or two way ANOVA. In figures (E-G, I, K) the data are plotted as linear regression. Source data are available online for this figure.

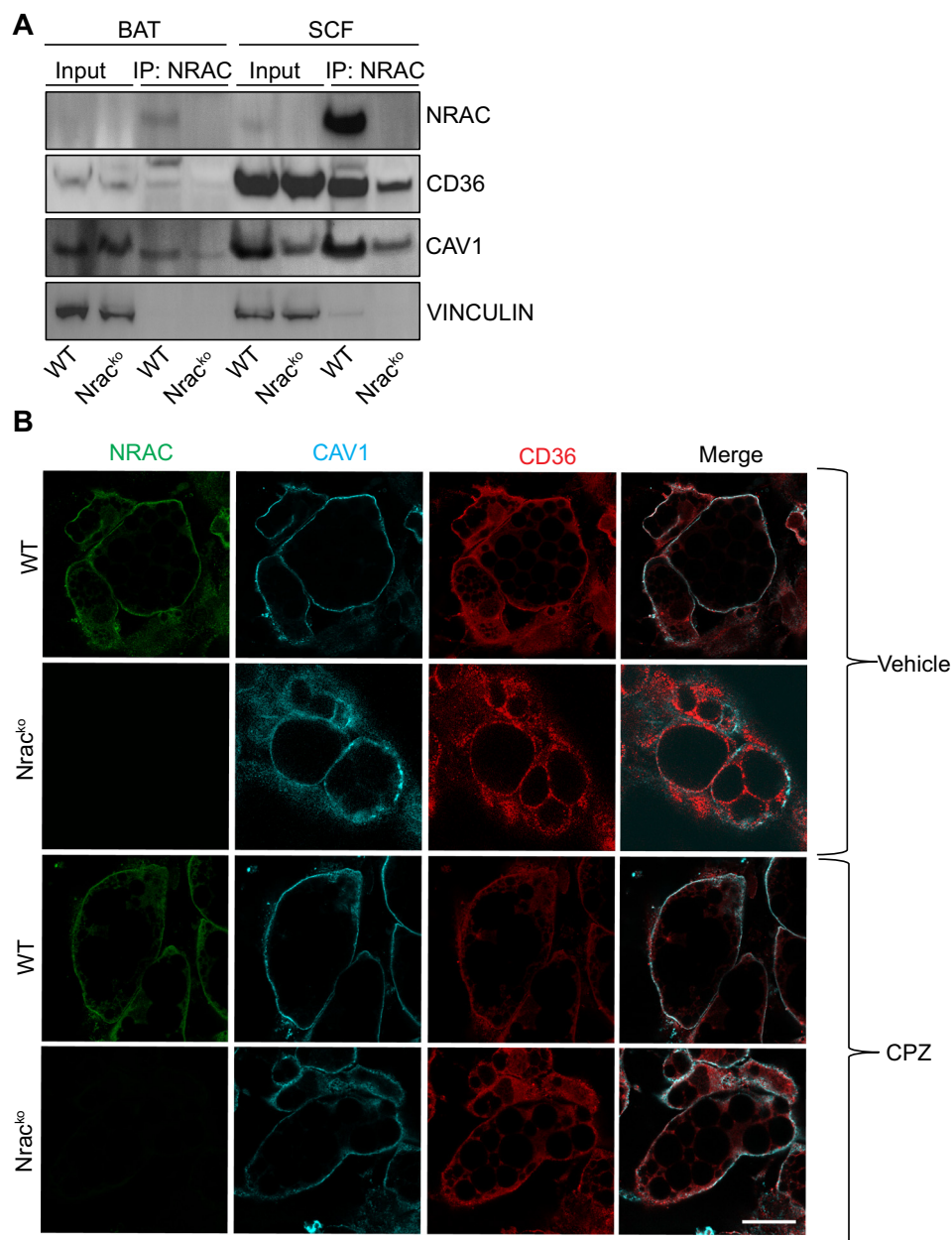


**Figure EV3. NRAC regulates CD36/Cav1 interaction in adipocytes.**

(A) Immunoprecipitation of NRAC from BAT and SCF. (B) Immunostaining of differentiated immortalized preadipocytes treated with vehicle (0.05% ethanol) or Chlorpromazine (CPZ) (10  $\mu$ M) for 1 h (scale 25  $\mu$ m). Source data are available online for this figure.

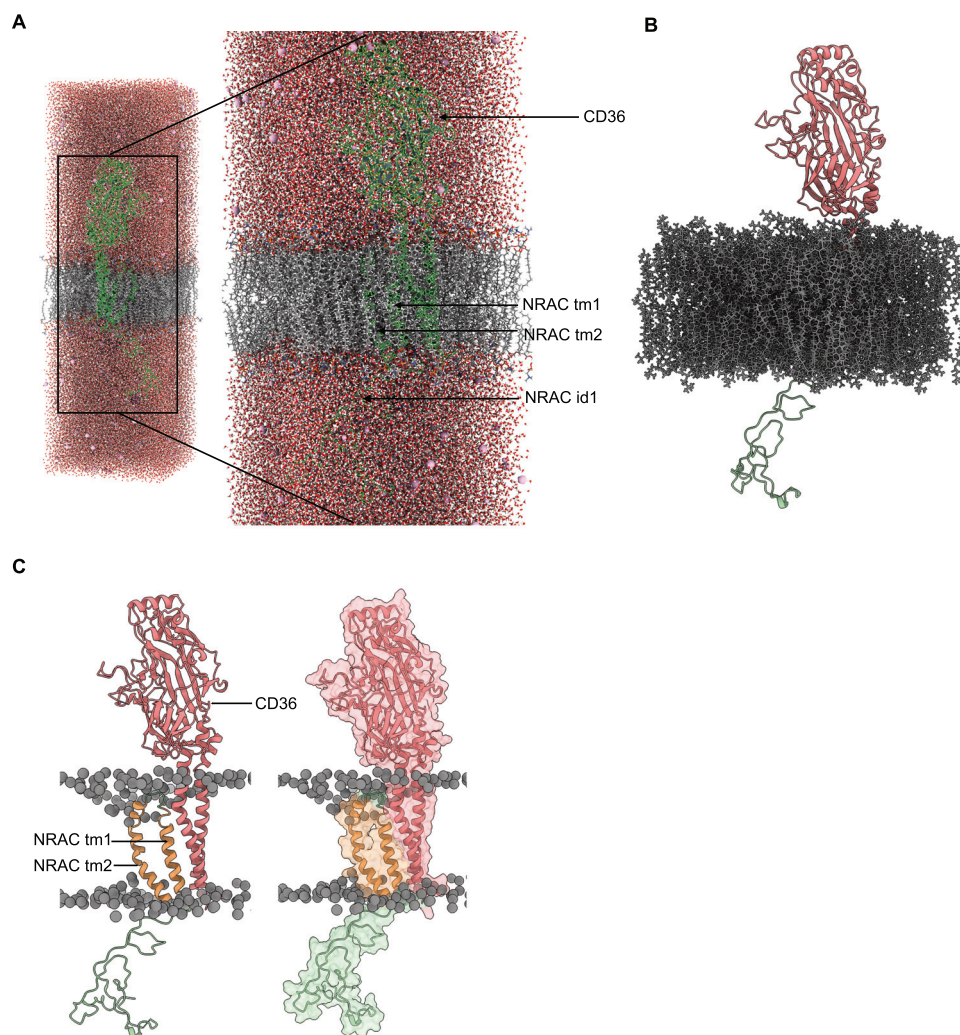
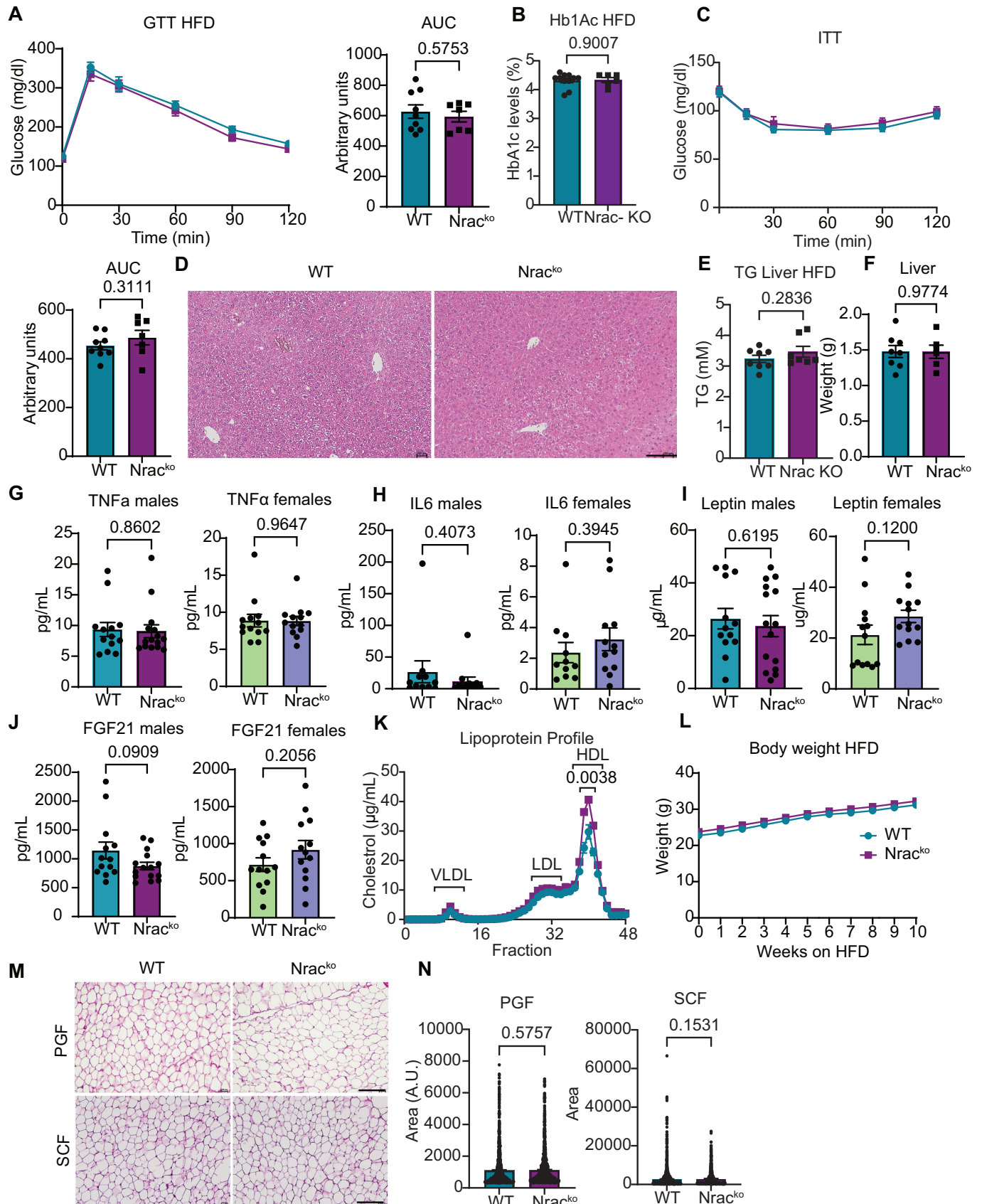


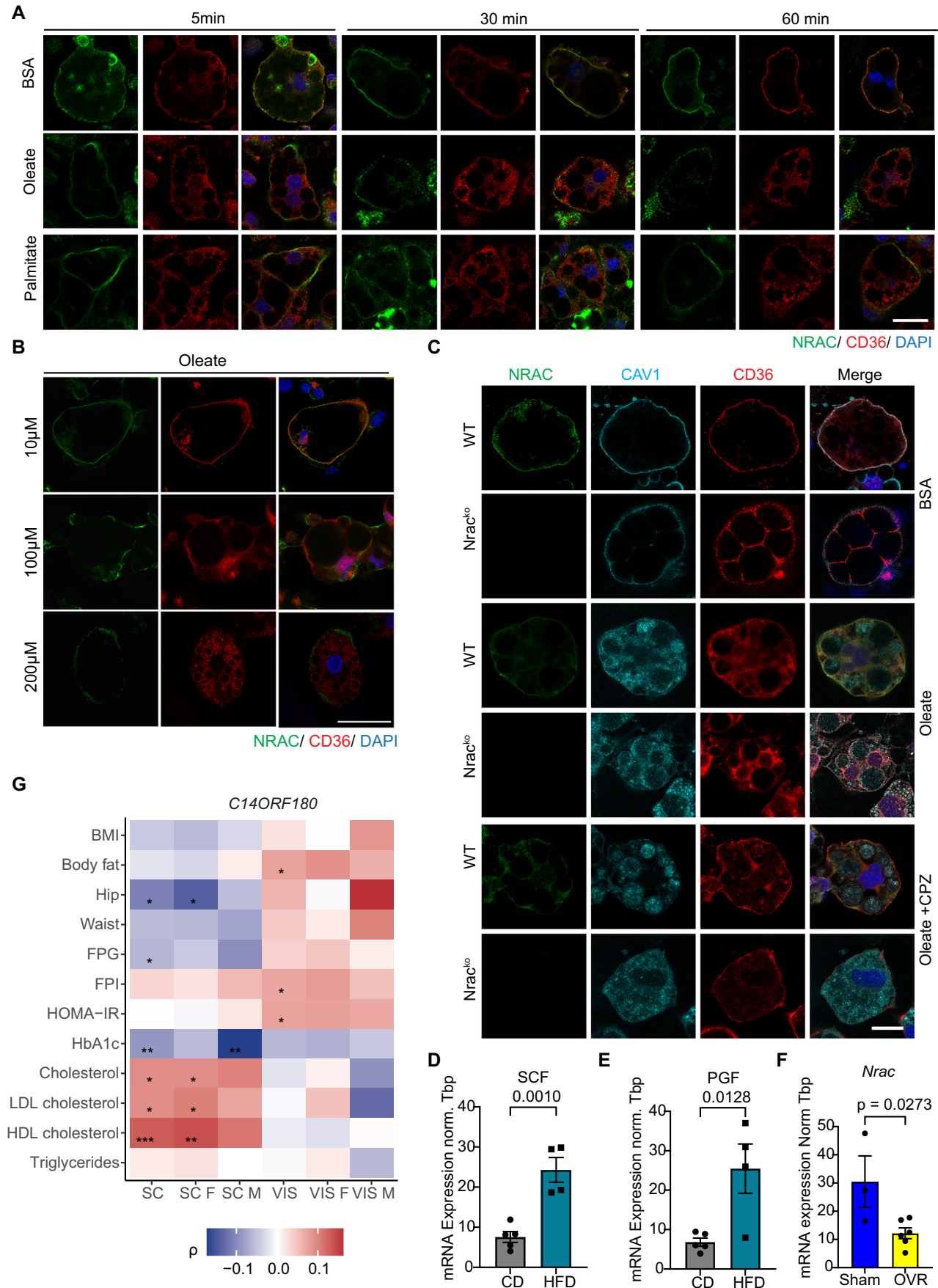
**Figure EV4. First transmembrane domain of NRAC is required for NRAC-CD36 interaction.**

(A) MD-simulations of human NRAC and CD36. The full simulation block is shown, with the central grey stripe representing the lipid bilayer membrane. Water molecules are depicted as red and white particles, while Na<sup>+</sup> and Cl<sup>-</sup> ions appear as pink spheres at a physiological concentration of 0.15 M. The bright green structures correspond to the proteins CD36 and NRAC, with CD36 embedded in the upper membrane leaflet and NRAC in the lower leaflet, and the zoomed in area of the same region. (B) CD36-NRAC complex is embedded in the membrane, with CD36 located on top and NRAC below. The membrane is shown in grey. (C) The CD36-NRAC complex is embedded in the membrane, with CD36 on top and NRAC below. Phospholipids in the membrane are represented as grey circles. Source data are available online for this figure.



◀ **Figure EV5. HFD feeding does not affect glucose metabolism, insulin sensitivity and plasma profile of inflammatory cytokines in *Nrac<sup>ko</sup>* mice.**

(A) Glucose tolerance test and baseline corrected area under the curve ( $n = 9$  wt, 7 ko, 10 weeks on HFD). (B) Percentage of HbA1c in mice 13 weeks on HFD ( $n = 9$  wt, 7 ko). (C) Insulin tolerance test and baseline corrected area under the curve, (12 weeks on HFD,  $n = 9$  wt, 7 ko). (D) H&E staining of livers of HFD fed mice (17 weeks on HFD), (E) Liver triglyceride levels and (F) liver weight ( $n = 9$  wt, 7 ko, 17 weeks on HFD), Plasma levels of (G) TNF $\alpha$ , (H) IL6, (I) Leptin, and (J) FGF21 in male and female non-fasted mice (male: 14 wt, 13 ko; female: 13 wt, 15 ko, 20 weeks on HFD). (K) Plasma lipoprotein profile ( $n = 5$  wt, 5ko, 10 weeks on HFD), (L) Body weight development in HFD fed animals ( $n = 8$  wt, 7 ko). Week 0 was the day when the diet was switched from chow to HFD (age 6 weeks). (M) H&E staining of PGF and SCF from HFD fed mice (17 weeks on HFD), and (N) the quantification of adipocyte cell size. Significance levels are indicated as follows: \* $P < 0.05$ , \*\* $P < 0.01$ , \*\*\* $P < 0.001$  by Student's  $t$  test in all figures except (A, C, K, L) where two-way ANOVA was used. Data are shown as mean  $\pm$  SEM. \* $P < 0.05$ , \*\* $P < 0.01$ , \*\*\* $P < 0.001$  by Student's  $t$  test in all figures except (A, C, K, L) where two-way ANOVA was used. Source data are available online for this figure.



◀ **Figure EV6. Fatty acid stimulation reduces NRAC surface localization in adipocytes.**

(A) Immunostaining of differentiated subcutaneous adipocytes, treated with BSA, Oleate (100  $\mu$ M) and palmitate (100  $\mu$ M) for 5, 30 and 60 min. On day 8 of differentiation, cells were starved with serum free medium for 1 h and treated with fatty acids for the indicated times. (B) Immunostaining of differentiated subcutaneous adipocytes on day 8 of differentiation. Cells were starved with serum free medium 1 h and treated with 10, 100 and 200  $\mu$ M BSA conjugated oleate. (C) Immunostaining of differentiated adipocytes treated either with oleate (100  $\mu$ M) or with oleate (100  $\mu$ M) and CPZ (10  $\mu$ M) for one hour after 1 h serum starvation. *Nrac* mRNA expression in (D) subcutaneous (SCF) and (E) perigonadal (PGF) adipose tissue from CD and HFD fed mice ( $n = 5$  CD and 4 HFD), (F) *Nrac* mRNA expression of sham and ovariectomized (OVR) HFD fed mice ( $n = 3$  sham, 6 ovariectomized). (G) The correlation of C14orf180 (human NRAC) gene expression with clinical parameters was analyzed in both subcutaneous (SC) and visceral (VIS) adipose tissue across all individuals, as well as separately for male (M) and female (F) participants. Spearman correlations were calculated, and *P* values were adjusted for false discovery rate. Significance levels are indicated as follows: \**P* < 0.05, \*\**P* < 0.01, and \*\*\**P* < 0.001. Data are shown as mean  $\pm$  SEM. \**P* < 0.05, \*\**P* < 0.01, \*\*\**P* < 0.001 by Student's *t* test in all figures except (A, C, K, L) where two-way ANOVA was used. Source data are available online for this figure.